Since January 2020 Elsevier has created a COVID-19 resource centre with free information in English and Mandarin on the novel coronavirus COVID-19. The COVID-19 resource centre is hosted on Elsevier Connect, the company's public news and information website.

Biotechnology Advances 59 (2022) 107986

Contents lists available at ScienceDirect

Biotechnology Advances

journal homepage: www.elsevier.com/locate/biotechadv

Research review paper

Native, engineered and *de novo* designed ligands targeting the SARS-CoV-2 spike protein

Carlos F.S. Costa [a,b], Arménio J.M. Barbosa [a,b], Ana Margarida G.C. Dias [a,b], Ana Cecília A. Roque [a,b,*]

[a] *Associate Laboratory i4HB – Institute for Health and Bioeconomy, School of Science and Technology, Universidade NOVA de Lisboa, 2829-516 Caparica, Portugal*
[b] *UCIBIO – Applied Molecular Biosciences Unit, Department of Chemistry, School of Science and Technology, Universidade NOVA de Lisboa, 2829-516 Caparica, Portugal*

ARTICLE INFO

Keywords:
SARS-CoV-2
Spike
ACE2
Affinity ligands
de novo design

ABSTRACT

The severe acute respiratory syndrome coronavirus 2 (SARS-CoV-2) is responsible for the deadly coronavirus disease 2019 (Covid-19) and is a concerning hazard to public health. This virus infects cells by establishing a contact between its spike protein (S-protein) and host human angiotensin-converting enzyme 2 (hACE2) receptor, subsequently initiating viral fusion. The inhibition of the interaction between the S-protein and hACE2 has immediately drawn attention amongst the scientific community, and the S-protein was considered the prime target to design vaccines and to develop affinity ligands for diagnostics and therapy. Several S-protein binders have been reported at a fast pace, ranging from antibodies isolated from immunised patients to *de novo* designed ligands, with some binders already yielding promising *in vivo* results in protecting against SARS-CoV-2. Natural, engineered and designed affinity ligands targeting the S-protein are herein summarised, focusing on molecular recognition aspects, whilst identifying preferred hot spots for ligand binding. This review serves as inspiration for the improvement of already existing ligands or for the design of new affinity ligands towards SARS-CoV-2 proteins. Lessons learnt from the Covid-19 pandemic are also important to consolidate tools and processes in protein engineering to enable the fast discovery, production and delivery of diagnostic, prophylactic, and therapeutic solutions in future pandemics.

1. Introduction

The coronavirus disease 2019 (Covid-19) is a major health concern that suddenly changed lives globally. By the 9th February 2022, approximately two years after the World Health Organisation had declared it a Public Health Emergency of International Concern, Covid-19 had caused the infection of over 403 M people and more than 5.78 M deaths globally (World Health Organization, 2021). Covid-19 is caused by the severe acute respiratory syndrome coronavirus 2 (SARS-CoV-2), a positive-sense single-stranded RNA virus of possible zoonotic origins, related to the SARS-CoV-1 and Middle East respiratory syndrome (MERS) virus (Machhi et al., 2020). SARS-CoV-2 is comprised of a spherical envelope with a diameter of 60–140 nm (Zhu et al., 2020), composed mainly of membrane and envelope proteins, as well as six different accessory proteins. Within the viral envelope, there are nucleocapsid proteins responsible for RNA packaging and release into host cells. In addition, the virus includes 16 non-structural proteins, such as proteases, helicase and RNA polymerase (Yoshimoto, 2020). Spike proteins (S-proteins) protrude from the spherical envelope, giving the virus the spiked appearance from which the name "coronavirus" derives. Each virus contains around 24–40 S-proteins at the surface (Scudellari, 2021). The S-protein is primarily responsible for binding to human angiotensin-converting enzyme 2 (hACE2) and, therefore, the S-protein has been immediately considered the prime target to design vaccines (Salvatori et al., 2020), diagnostics and therapies (Renn et al., 2020). Within the field of therapeutics, several efforts are being made to bring to the market neutralising ligands to treat the disease or attenuate its symptoms, as a prophylactic approach, by mimicking the immune response through binding to the virus and impeding its replication. These neutralising ligands include antibody clones isolated from peripheral blood mononuclear cell (PBMC) samples (Yuan et al., 2020a) or discovered through *in vitro* evolution (Bertoglio et al., 2021), as well as

* Corresponding author at: Associate Laboratory i4HB – Institute for Health and Bioeconomy, School of Science and Technology, Universidade NOVA de Lisboa, 2829-516 Caparica, Portugal.
E-mail address: cecilia.roque@fct.unl.pt (A.C.A. Roque).

https://doi.org/10.1016/j.biotechadv.2022.107986
Received 14 September 2021; Received in revised form 29 April 2022; Accepted 16 May 2022
Available online 19 May 2022

engineered bispecific antibodies (De Gasparo et al., 2021). There are also alternative scaffold ligands, namely peptides discovered by evolution (*e.g.* cyclic peptides) (Norman et al., 2020), *de novo* designed decoys and proteins without an antibody scaffold (Cao et al., 2020a; Linsky et al., 2020). A reverse approach consisting of targeting hACE2 using S-protein-based rationally evolved small proteins, instead of the opposite, has also been demonstrated effective in inhibiting infection by blocking hACE2 access for the virus' S-proteins (Zahradník et al., 2021). Taken together, these approaches highlight the power of peptide and protein design and engineering, namely for the implementation of efficient therapies for SARS-CoV-2 and its variants (Wang et al., 2021a), either used alone or in combination (Renn et al., 2020).

The molecular recognition aspects of the interaction between the target S-protein and its respective ligands are one of the fundamental aspects for the successful development of molecules to reach the clinic. Therefore, in this review, we provide an overview of S-protein ligands – peptide and protein ligands – as well as the identification of several S-protein interaction hot spots, which can be useful to further design efficient S-protein binders.

The structural information released throughout the year of 2020 on the complexes formed between the SARS-CoV-2 S-protein and different ligands was compiled and analysed in depth. All SARS-CoV-2 S-protein structures (UniProt accession code P0DTC2) released on the Protein Data Bank (PDB) until the 1st January 2021 were included for this analysis. In total, 197 structures were considered, of which 68 represent the S-protein alone and 129 correspond to complexes of the S-protein with at least one ligand.

The structures of the S-protein in complex with ligands were then categorised based on the type of ligand: i) native ligand, hACE2; and alternative ligands, namely ii) antibody antigen-binding fragment (Fab) fragments, iii) single-domain antibody fragments and iv) *de novo* designed peptide scaffolds. For each complex with a structure available in the PDB, the following information was collected: ligand sequence, structure determination technique, origin, method of production and binding affinity. The information was gathered from the respective literature and compiled into a database, which is available in (Costa et al., 2021). It should be noted that affinity constants have been measured using different methodologies, namely bio-layer interferometry (BLI), isothermal titration calorimetry (ITC), surface plasmon resonance (SPR), or enzyme linked immunosorbent assay (ELISA), which may influence the correct comparison and overview of all systems.

In addition, since the date of retrieval of the structures analysed in depth (1st January 2021) until January 2022, 555 more structures of the SARS-CoV-2 S-protein were released in the PDB, 411 of which in complex with a ligand: 79 with hACE2, 274 with Fab fragments, 56 with single-domain antibody fragments and 2 with *de novo* designed peptide scaffolds.

In this review, we looked into detail over 25 X-ray and cryo-EM structures of the S-protein bound to hACE2 released in the PDB until the 1st January 2021 (Costa et al., 2021). In these structures, all important intermolecular interactions were analysed using molecular visualisation software PyMOL 2.4.1. Polar interactions such as hydrogen bonds and salt bridges were considered within distances between heavy atoms of up to 3.6 Å, and hydrophobic and π interactions up to 6.0 Å (Bissantz et al., 2010). This method of analysis was extended to 106 X-ray, NMR and cryo-EM structures in which the S-protein is in complex with at least one alternative ligand, also released in the PDB until the 1st January 2021 (Costa et al., 2021). In more detail, the 106 S-protein in complex with alternative ligand structures included: 85 complexes with Fab fragments, 18 with single-domain antibody fragments and 5 with *de novo* designed peptide scaffolds.

2. Analysis of ligands targeting SARS-CoV-2 spike protein

2.1. Human ACE2 as the native spike protein ligand

The trimeric S-protein exhibits a molecular weight of 180–200 kDa and possesses 1273 amino acids per chain (Huang et al., 2020). It is comprised of two subunits, S1 and S2. The S1 subunit (residues 1–685) is the farthest from the viral envelope and interacts with hACE2 through a specific region designated the receptor-binding domain (RBD; residues 319–541). This domain can change between a "down" and an "up" conformation. In the "down" conformation, the RBD folds inwards the S-protein, whereas, in the "up" conformation, the RBD extends outwards (Wrapp et al., 2020) and exposes the residues which interact with hACE2, most of which are found in a small segment of the RBD denominated the receptor-binding motif (RBM; residues 437–508). In fact, an RBD can only interact with hACE2 in the "up" conformation (Fig. 1D). Each S-protein presents one RBD in the "up" conformation at a time (Fig. 1A), as it impacts its structural stability (Moreira et al., 2020). Once bound to hACE2, the S1 subunit is cleaved from S2 either by host transmembrane protease serine 2 (TMPRSS2) or endosomal cathepsins B and L (CatB/L). Unhindered by S1, the S2 subunit (residues 686–1273) initiates viral fusion and cell entry. Spontaneous dissociation of S1 from S2 can also occur. However, the resulting exposed S2 subunits do not interact with cells and have a possible protective role, sheltered by N-linked glycans to avoid triggering an immune response (Cai et al., 2020).

About 26 hACE2 residues, located in two of its α-helices, interact with about 22 S-protein residues, almost all of which pertaining to the RBM. These complexes possess estimated dissociation constants (K_D) ranging from 4.7 nM (Lan et al., 2020) to 94.6 nM (Wang et al., 2020), depending on the pH and method of measurement, as well as on the type of target used (the whole S-protein, just the S1 subunit or the RBD only). It was observed that these interactions are concentrated in two hot spots around hACE2 residues K31 and K353 which interact strongly with RBD residues Q493 and Q498-Y505, respectively (Wan et al., 2020; Veeramachaneni et al., 2020; Ghorbani et al., 2020). These two hACE2 lysine residues complement their interaction with the RBD with neighbouring residues (Fig. 3). It is also interesting to note that the S-protein is heavily glycosylated (Watanabe et al., 2020), yet the amino acids interacting with the hACE2 are not glycosylated and are highly accessible for interaction (Fig. 1C and E).

Mutations in SARS-CoV-2 gave rise to five variants of concern, the α (B1.1.1.7), β (B.1.351), γ (P.1), δ (B.1.617.2) and ο (omicron) (B1.1.529) variants. Several mutations occur in the S-protein, which were reviewed here in more detail. The cryo-EM structures of the mutated S-proteins alone and in complex with hACE2 for all the current five variants of concern have been released at a fast pace. To summarise the differences, the mutated S-protein residues of the α, β, γ, δ and ο variants were mapped in the structure and chain representations of a wild-type S-protein (Figs. 1A, B and 2). For all variants of concern except ο, despite some mutations occurring at the RBD, and even within the RBM, this region is comparatively more conserved than other domains of the S-protein, such as the N-terminal domain (NTD), where more mutations are observed. Regarding the ο variant, which is the variant with the highest number of mutations to date, out of 32 mutations on the S-protein, 15 occur at the RBD and 10 within the RBM (Fig. 2). Despite this, recent studies show that the ο variant S-protein actually binds with higher affinity to hACE2 than the original strain S-protein (Rath et al., 2021; Shah and Woo, 2021), with a binding affinity comparable to that of the δ variant (Hong et al., 2022). In fact, the RBD of all variants of concern bound with higher affinity to hACE2 than the original strain RBD, with the α, β and γ variants showing a 7-, 3- and 5-fold increase in binding strength (Han et al., 2021). Still, it should be noted that the K_D values are determined by various techniques and against distinct targets, namely the whole S-protein, the S1 subunit or the RBD only. This further emphasises the need to develop competitors for this specific interaction as potential therapeutic agents against SARS-CoV-2.

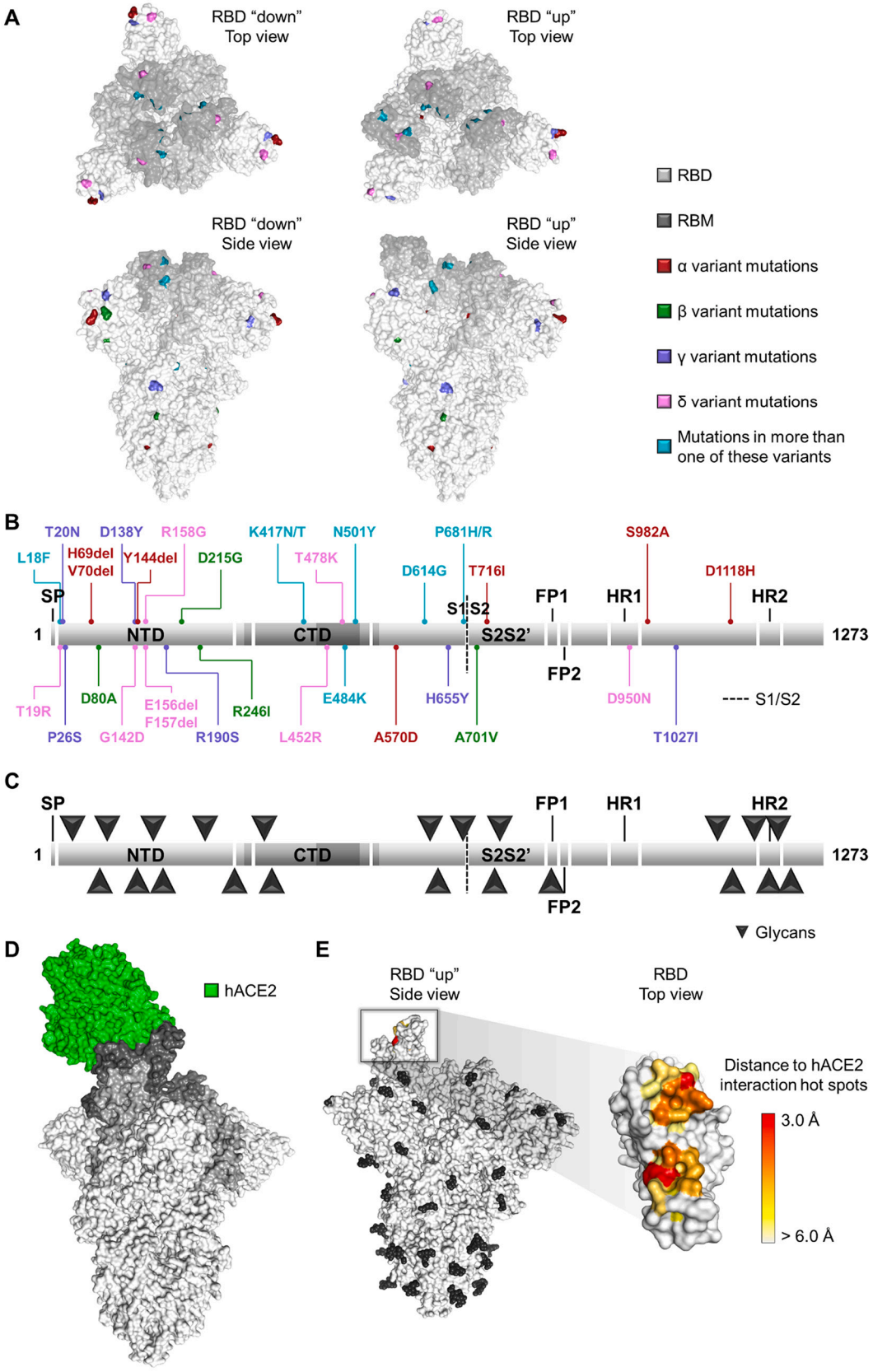

(caption on next page)

Fig. 1. Structure and sequence of the SARS-CoV-2 S-protein. **(A)** The receptor-binding domains (RBD) (light grey) and receptor-binding motifs (RBM) (dark grey). Top view (top) and side view (bottom) of the trimeric S-protein with all RBD "down" (left) (PDB 7KDG) and with one RBD "up" (right) (PDB 7KDH). Residues mutated in the α variant (dark red), in the β variant (dark green), in the γ variant (slate blue), in the δ variant (violet) and common to more than one variant (teal). The same colour code applied to the rest of the fig. **(B)** Schematic representation of the S-protein sequence and its domains: signal peptide (SP), N-terminal domain (NTD), C-terminal domain (CTD), S1/S2 cleavage site to S2' (S2S2'), fusion peptide 1 (FP1), fusion peptide 2 (FP2), heptad repeat 1 (HR1) and heptad repeat 2 (HR2). In the CTD region, the RBD cores and RBM are highlighted. The cleavage site between subunits S1 and S2 is indicated (dashed line). Residues mutated in the variants are identified as in (A). Deletions in S-protein are identified as H69del, V70del and Y144del. Mutation L18F is common to the β and γ variants; K417 mutates to N in the β and γ variants, although it has been reported to also mutate to T in the γ variant; E484 mutates to K in the β and γ variants and to Q in the δ variant; N501Y is common to the α, β and γ variants; D614G is common to the β and δ variants; P681 mutates to H in the α variant and to R in the δ variant. **(C)** Schematic representation of S-protein glycosylation sites. **(D)** Structure of an original strain S-protein with one RBD "up" bound to native ligand hACE2 (green) (PDB 7DF4). The RBD cores and RBM are highlighted. **(E)** Structure of an original strain S-protein in the "up" conformation with all glycosylation sites filled (glycans represented in black) and with the hACE2 binding site in a gradient of residue proximity to hACE2 interaction hot spots (PDB 7DF4). (For interpretation of the references to colour in this figure legend, the reader is referred to the web version of this article.)

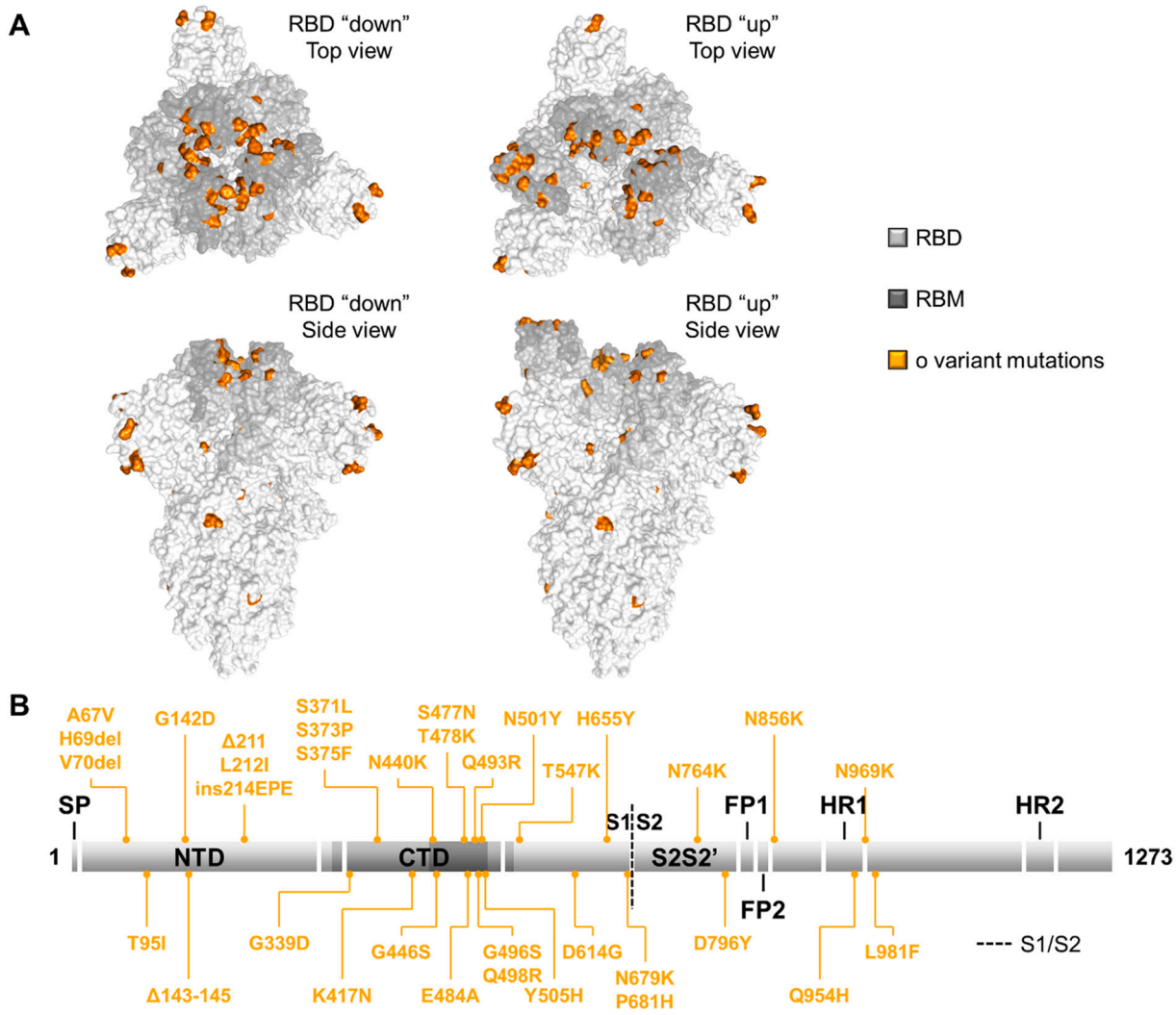

Fig. 2. Structure and sequence of the SARS-CoV-2 o variant S-protein. **(A)** The receptor-binding domains (RBD) (light grey) and receptor-binding motifs (RBM) (dark grey). Top view (top) and side view (bottom) of the trimeric S-protein with all RBD "down" (PDB 7KDG, left) and with one RBD "up" (PDB 7KDH, right). RBD and RBM cores highlighted, as well as residues mutated in the variant o (orange). **(B)** Schematic representation of the S-protein sequence and its domains. Residues mutated in the o variant are identified as in (A). Deletions in S-protein are identified as H69del and V70del. Insertions are identified as ins214EPE.

To highlight important structural differences in the contacts established between the SARS-CoV-2 S-protein RBD and hACE2 across the five variants of concern, the structures of the original strain and mutant S-protein with one RBD "up" in complex with hACE2 are summarised in Fig. 3. By comparing the mutated residues to those in the original strain protein, it is suggested that potentially stronger interactions with ligands could occur in the variant S-proteins, which is in accordance with experimental data that determined higher binding affinities between hACE2 and the five variants (Hong et al., 2022; Han et al., 2021). For instance, the RBD residue N501, which is in close proximity to hACE2 interaction hot spot K353 (Wan et al., 2020; Veeramachaneni et al., 2020; Ghorbani et al., 2020), is replaced by a tyrosine in all variants of concern except δ, which shortens the distance to hACE2 K353 and establishes a greater number of contacts with its neighbouring residues (PDB 7EKF for α and 7EKG for β (Han et al., 2021), 7V84 for γ, 7V8B for δ and 7T9L for o variants bound to hACE2).

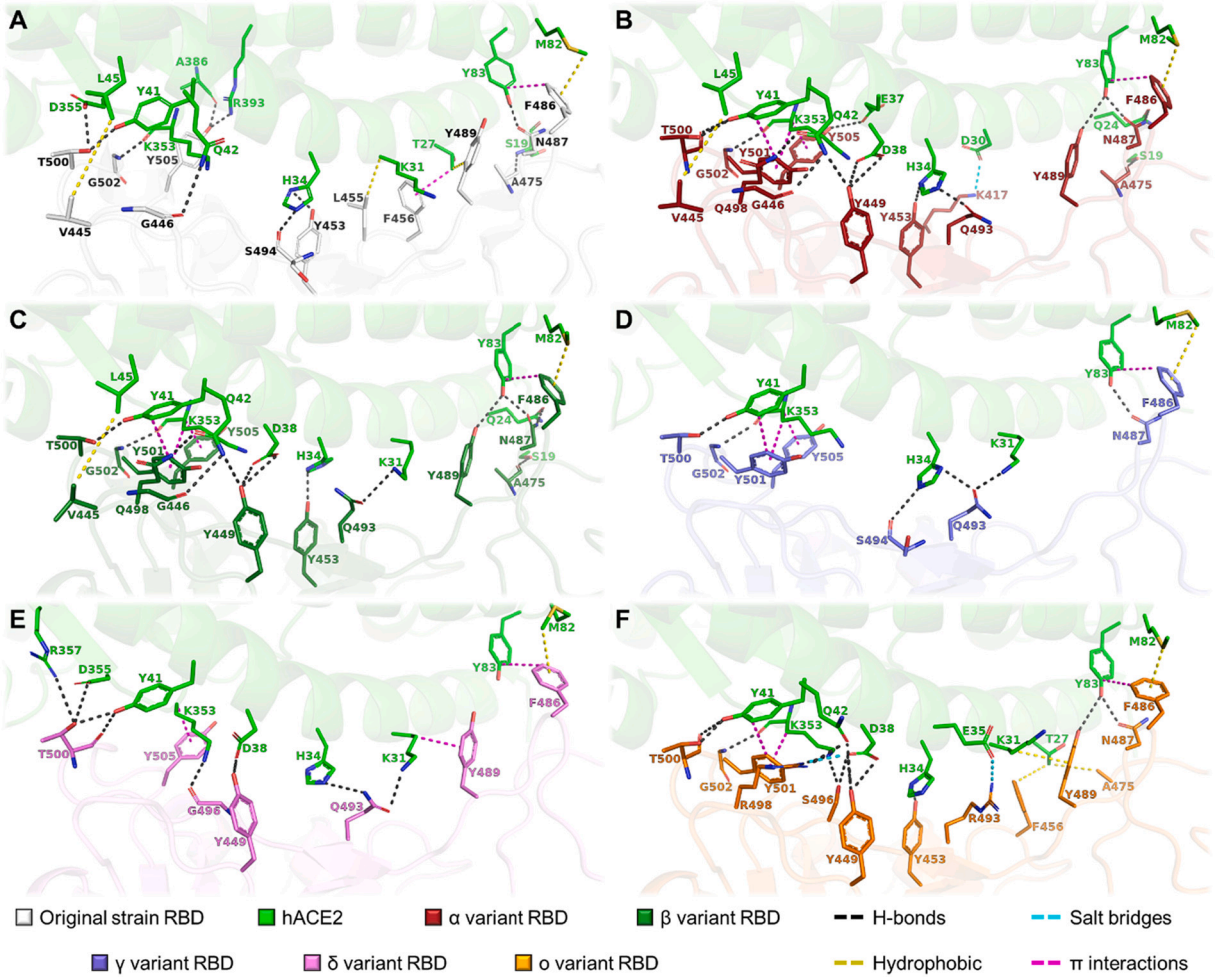

Fig. 3. Intermolecular interactions between the native ligand hACE2 (green) and the RBD pertaining to the **(A)** original strain (white) (PDB 7DF4), **(B)** α variant (dark red) (PDB 7EKF), **(C)** β variant (dark green) (PDB 7EKG), **(D)** γ variant (slate blue) (PDB 7V84), **(E)** δ variant (violet) (PDB 7V8B) and **(F)** ο variant (orange) (PDB 7T9L). Hydrogen bonds are represented as black dashed lines, salt bridges as cyan, hydrophobic interactions as yellow and π interactions as magenta. (For interpretation of the references to colour in this figure legend, the reader is referred to the web version of this article.)

Comparing the intermolecular interactions between hACE2 and the RBD of original strain and variant of concern S-proteins (Fig. 3), it was possible to observe an increase in the number of contacts surrounding the two interaction hot spots mentioned in the literature, as well as hACE2 residue H34. This higher density of contacts in the aforementioned regions is more noticeable in the α, β and ο variants. Furthermore, there is an apparent tendency towards more of the stronger types of interactions being established in the variants, namely the increase in hydrogen bonds and the appearance of a few salt bridges.

The structure of the ο variant S-protein in complex with hACE2 has also been analysed in depth in (Mannar et al., 2022), which reported new hydrogen bonds and salt bridges formed by RBD mutated residues R493, S496 and R498 with hACE2, thus increasing binding affinity. These observations are in agreement with our structural analysis of this variant.

2.2. *Alternative S-protein ligands*

Since the dawn of the Covid-19 pandemic, several efforts were made to find S-protein binders other than the hACE2. In this second section, the structural features of the complexes formed between the S-protein and alternative ligands are detailed. Alternative S-protein ligands were

Table 1
Comparison between the different S-protein alternative ligands.

Ligand type	No. of different ligands	No. of available structures	K_D range (nM)	Origin	Production
Antibody Fab fragments	48	85	<0.001–313	Human antibodies against MERS or SARS-CoV-1; SARS-CoV-2-specific antibodies from immunised humans, apes, or mice	Mammalian cells (*e.g.* HEK 293 cells; CHO cells)
Single-domain antibody fragments	11	18	<0.001–210	Discovery by panning llama single-domain antibodies libraries against the SARS-CoV-2 spike protein or RBD	Mammalian cells (*e.g.* HEK 293 cells) and bacterial hosts (*e.g. E. coli* BL21(DE3) cells)
De novo designed peptide scaffolds	3	5	<1–21	Rationally designed, either inspired on hACE2 or from scratch using rotamer interaction field (RIF) docking	*E. coli* Bacterial hosts

categorised as antibody antigen-binding fragment (Fab) fragments (recently revised (Du et al., 2021)), single-domain antibody fragments and *de novo* designed peptide scaffolds. Table 1 and Fig. 4 summarise the information collected from the structures of complexes between S-protein and ligands. For detailed information on the sequence of the ligands shown in Fig. 4, please refer to Table 2.

Anti-S-protein antibodies were mainly obtained through the isolation of antibody clones from PBMC samples from humans, apes or mice immunised against the MERS virus, SARS-CoV-1 or SARS-CoV-2 (Yuan et al., 2020a; Liu et al., 2020a; Rujas et al., 2020; Acharya et al., 2020; Zhang et al., 2021; Wu et al., 2020a; Cao et al., 2020b; Du et al., 2020; Barnes et al., 2020a; Barnes et al., 2020b; Shi et al., 2020; Yuan et al., 2020b; Wu et al., 2020b; Kreye et al., 2020; Hurlburt et al., 2020; Wang et al., 2021b; Yao et al., 2021; Ju et al., 2020; Hansen et al., 2020; Tortorici et al., 2020; Piccoli et al., 2020; Zhou et al., 2020; Liu et al., 2020b; Lv et al., 2020). The corresponding Fab fragments (around 50 kDa) were subcloned and used to generate S-protein ligands. Compared to the other categories of S-protein binders, Fab fragments exhibited a broad range of binding affinities to the SARS-CoV-2 S-protein, from below 0.001 nM to 313 nM (Fig. 6B). For instance, CR3022, a Fab specific against SARS-CoV-1, bound to the SARS-CoV-2 S-protein RBD with a K_D of 115 nM, measured using BLI (Yuan et al., 2020a). The 2G12 Fab, which is specific against HIV-1, bound to the SARS-CoV-2 S-protein S2 subunit with a K_D of 313 nM, determined by SPR (Acharya et al., 2020). Despite the high homology between the S-proteins of SARS-CoV-1 and SARS-CoV-2 (76.04%, calculated using the blastp tool at the NCBI website), the binding of ligands developed for SARS-CoV-1 were of limited use (Yuan et al., 2020a). On the other extreme, the P17, REGN10933 and REGN10987 Fabs bound to the S-protein with very high affinity (K_D between 0.04 nM and 0.096 nM), and are further detailed here.

Several single-domain antibody fragments have been discovered by *in vitro* screening of llama variable heavy chain of heavy-chain antibody (VHH) libraries against SARS-CoV-2 antigens, namely the S-protein and RBD (Schoof et al., 2021; Xiang et al., 2021; Custódio et al., 2020; Hanke et al., 2020; Bracken et al., 2020).

De novo designed peptide scaffolds (6–17 kDa) include hACE2 decoys and computationally-derived structures designed to bind with high affinity to the S-protein RBD, namely to the hACE2 binding site (Cao et al., 2020a; Linsky et al., 2020).

The structures of representatives of each ligand type and their interactions with the S-protein are illustrated in Figs. 4 and 5D–G, respectively. Specifically, the P17 Fab fragment and the Ty1 VHH fragment were chosen due to their high binding affinities to the S-protein (P17 bound to the RBD with a K_D of 0.096 nM, determined by SPR (Yao et al., 2021); and Ty1 bound to the RBD with a K_D of 5–10 nM, measured using BLI (Hanke et al., 2020)), the fact that both bind to the hACE2 binding site in the RBD, as well as the completeness of the sequences and high resolution of the structures. Thus, these ligands allowed a more accurate comparison between the interacting residues of natural and alternative ligands.

2.3. Binding sites of alternative S-protein ligands

As SARS-CoV-2 can only enter a cell if one of its S-proteins binds to hACE2, interfering with this interaction is a way to halt infection. As such, most S-protein ligands known to date have been developed with the aim to halt infection by directly competing with hACE2 binding to RBD (Figs. 5 and 6). Still, there are ligands targeting different surface regions of the S-protein which can cause steric hindrance effects or impede the RBD from assuming an “up” conformation. A few of the analysed structures bind to other S-protein domains, namely the NTD

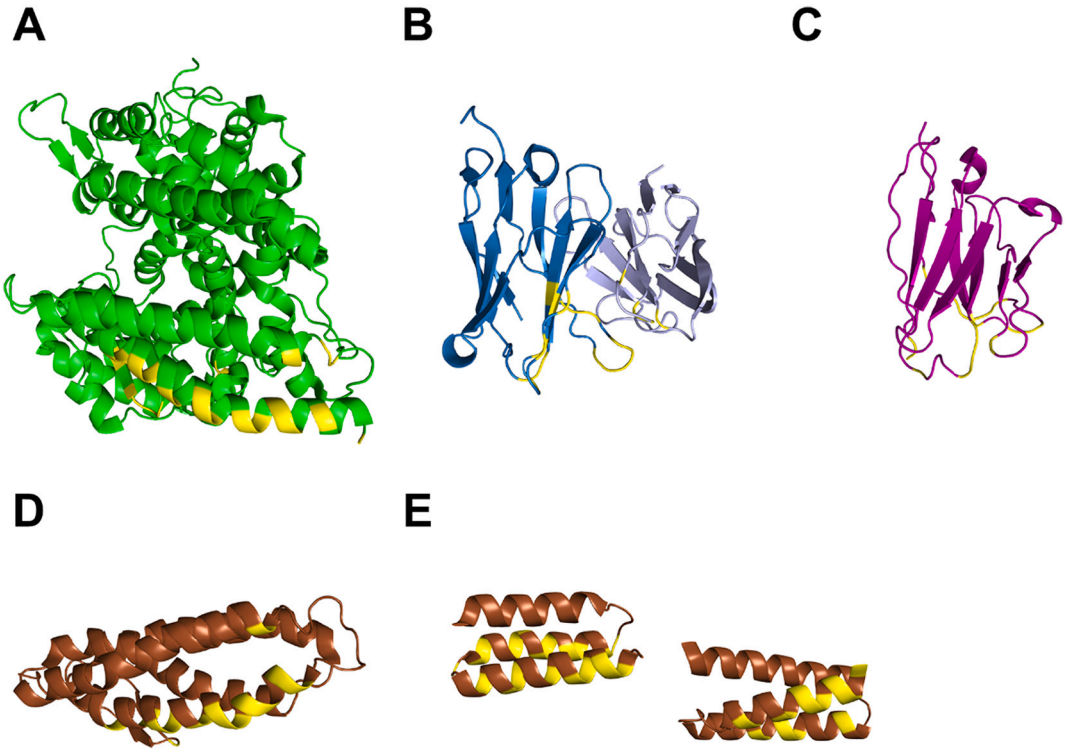

Fig. 4. Structures of SARS-CoV-2 S-protein ligands. Natural ligand: **(A)** hACE2 (PDB 7DF4; total 625 residues, of which 597 are visible in this structure); alternative ligands: **(B)** P17 Fab antibody fragment (PDB 7CWM; 120 residues in the heavy chain; 108 in the light chain); **(C)** Ty1 VHH antibody fragment (PDB 6ZXN; total 134 residues, of which 118 are visible in this structure); **(D)** *de novo* designed peptide hACE2 decoy CTC-445.2 (PDB 7KL9; 160 residues); and **(E)** *de novo* designed mini-inhibitors LCB1 (top; PDB 7JZU; 55 residues) and LCB3 (bottom; PDB JZM; total 106 residues, of which 64 are visible in this structure). Residues contacting with the S-protein are highlighted (yellow) in the structures and identified in the sequences in bold and underlined in Table 2. (For interpretation of the references to colour in this figure legend, the reader is referred to the web version of this article.)

Table 2
Sequences of selected S-protein ligands with interacting residues marked in bold and underlined.

Ligand type	Ligand name	Ligand sequence
Native	hACE2	1 STIEEQAKTFLDKFNHEAEDLFYQSSLASWNYNTNITEEN 41 VQNMNNAGDKWSAFLKEQSTLAQMYPLQEIQNLTVKLQLQ 81 ALQQNGSSVLSEDKSKRLNTILNTMSTIYSTGKVCNPDNP 121 QECLLLEPGLNEIMANSLDYNERLWAWESWRSEVGKQLRP 161 LYEEYVVLKNEMARANHYEDYGDYWRGDYEVNGVDGYDYS 201 RGQLIEDVEHTFEEIKPLYEHLHAYVRAKLMNAYPSYISP 241 IGCLPAHLLGDMWGRFWTNLYSLTVPFGQKPNIDVTDAMV 281 DQAWDAQRIFKEAEKFFVSVGLPNMTQGFWENSMLTDPGN 321 VQKAVCHPTAWDLGKGDFRILMCTKVTMDDFLTAHHEMGH 361 IQYDMAYAAQPFLLRNGANEGFHEAVGEIMSLSAATPKHL 401 KSIGLLSPDFQEDNETEINFLLKQALTIVGTLPFTYMLEK 441 WRWMVFKGEIPKDQWMKKWWEMKREIVGVVEPVPHDETYC 481 DPASLFHVSNDYSFIRYYTRTLYQFQFQEALCQAAKHEGP 521 LHKCDISNSTEAGQKLFNMLRLGKSEPWTLALENVVGAKN 561 MNVRPLLNYFEPLFTWLKDQNKNSFVGWSTDWSPYAD 597
Fab fragment	P17	Heavy chain: 1 QQLVESGGGVVQPGRSLRLS 21 CAASGFTFSSYAMHWVRQAP 41 GKGLEWVAVISYDGSNKYYA 61 DSVKGRFTISRDNSKNTLYL 81 QMNSLRAEDTAVYYCARHAT 101 LMNNKDIWGQGTLVTVSSAS Light chain: 1 GDIQLTQSPSSLSASVGDRV 21 TITCRASQSISSYLNWYQQK 41 PGKAPKLLIYAASSLQSGVP 61 SRFSGSGSGTDFTLTISSLQ 81 PEDFATYYCQQSYSTPRTFG 101 QGTKVEIK 108
Single-domain antibody fragment	Ty1	1 QVQLVETGGGLVQPGGSLRLSCAASGFTFSSVYMNWVRQA 41 PGKGPEWVSRISPNSGNIGYTDSVKGRFTISRDNAKNTLY 81 LQMNNLKPEDTALYYCAIGLNLSSSSVRGQGTQVTVSS 118
De novo designed peptide scaffolds	CTC-445.2	1 SAEIDLGKGDFREIRASEDAREAAEALAEAARAMKEALEI 41 IREIAEKLRDSSRASEAAKRIAKAIRKAADAIAEAAKIAA 81 RAAKDGDAARNAENAARKAKEFAEEQAKLADMYAELAKNG 121 DKSSVLEQLKTFADKAFHEMEDRFYQAALAVFEAAEAAAG
	LCB1	1 DKEWILQKIYEIMRLLDELGHAEASMRVSDLIYEFMKKGD 41 ERLLEEAERLLEEVE 55
	LCB3	1 NDDELHMLMTDLVYEALHFAKDEEIKKRVFQLFELADKAY 41 KNNDRQKLEKVVEELKELLERLLS 64

region (the 4A8 Fab fragment (Chi et al., 2020)) or the S2 subunit (the 2G12 Fab fragment (Williams et al., 2021). Recently, interest has grown in ligands that target the more inaccessible regions of the S-protein, such as the S2 subunit, which is overall more conserved than S1 and, therefore, less prone to mutations that lead to viral immune evasion. These ligands can potentially be useful for diagnostics, therapy or vaccine design (epitopes as immunogens), as recently highlighted (Shah et al., 2021).

Focusing our attention on alternative ligands binding at the RBD, it became evident, by superimposing all structures of S-protein complexes, that RBD binding is not limited to the same spots found for the natural ligand hACE2 (Fig. 5A–C, and (Costa et al., 2021)). Some RBD-binding antibody fragments do not bind to the RBM, but to the RBD core, therefore they have the possibility of binding to the S-protein even when all RBD are in the "down" conformation. Overall, it was possible to identify five recurrent binding sites in the S-protein. We identified as binding site 1 the region where hACE2 binds, which essentially comprises the RBM. Binding sites 2 to 5 involve residues mainly outside the RBM and upstream on the sequence. Binding sites 4 and 5 comprise a region that remains completely accessible even in the "down" conformation, whereas binding site 2 becomes only partly accessible due to some steric hindrance from the S-protein NTD. In contrast, binding site 3 is located on a region of the RBD which faces inwards in the "down" conformation, becoming completely inaccessible.

2.4. Evaluating alternative ligands targeting the hACE2 binding site

Considering that binding site 1 is clearly the most prevalent amongst alternative S-protein ligands, the structural details of the interaction between the S-protein and alternative ligands targeting binding site 1 were analysed for three exemplificative PDB structures with the highest resolution (details in Costa et al. (2021)) and compared with hACE2 interaction (Fig. 5D–G, Table 2 and (Costa et al., 2022)).

In more detail, the P17 Fab binds to the RBM, however slightly more upstream in the S-protein chain when compared to hACE2, whilst interacting with a narrower area of the RBM. For instance, the P17 Fab does not interact with RBM residues 498–505, which are within proximity of hACE2 interaction hot spot K353 (Veeramachaneni et al., 2020). Despite this, and even though the P17 Fab interacts with only 13 RBM residues, it binds to the S-protein with very high affinity (K_D = 0.096 nM, determined by SPR) (Yao et al., 2021). Similarly, the REGN10933 and REGN10987 Fabs (PDB 6XDG) bind each to a different

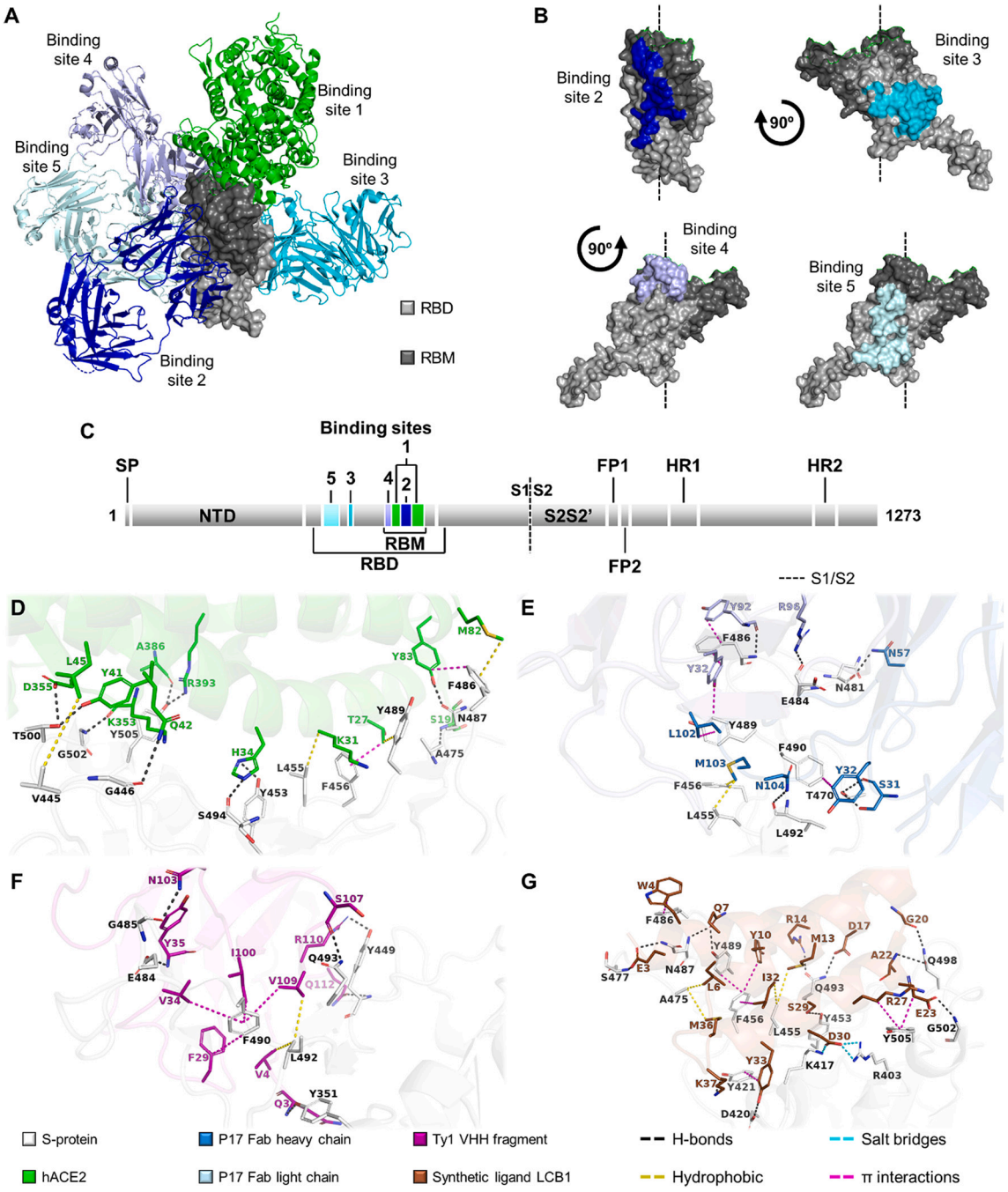

Fig. 5. Characterisation of S-protein binding sites located in the RBD. **(A)** Summary of the RBD binding sites, with a representative ligand bound to each. **(B)** Frontal and side views of the RBD with the residues from each binding site highlighted in their respective colours, as in (A). **(C)** Loci of each binding site highlighted in the schematic representation of the S-protein chain. Intermolecular interactions between the original strain RBD and the representative ligands of each type categorised in this analysis: **(D)** native ligand hACE2 (PDB 7DF4); **(E)** antibody Fab fragments (represented by the P17 antibody Fab; PDB 7CWM); **(F)** Single-domain antibody fragments (represented by the Ty1 VHH fragment; PDB 6ZXN); and **(G)** *de novo* designed peptide scaffolds (represented by the synthetic ligand LCB1; PDB 7JZL). Hydrogen bonds are represented as black dashed lines, salt bridges as cyan, hydrophobic interactions as yellow and π interactions as magenta. (For interpretation of the references to colour in this figure legend, the reader is referred to the web version of this article.)

short RBM region, with REGN10933 binding more downstream than REGN10987 in the S-protein sequence. Both Fab molecules have been demonstrated to bind simultaneously without causing steric hindrance and with very high binding affinities (K_D = 0.0417 nM for the REGN10933 Fab and K_D = 0.0428 nM for the REGN10987 Fab, both measured using SPR) (Hansen et al., 2020). The EY6A Fab (PDB 6ZCZ, 6ZDG, 6ZDH, 6ZER and 6ZFO) does not target the RBM, but instead interacts with residues 369–430 and 517, in the RBD core. Despite not competing directly with hACE2, it binds very strongly (K_D = 2 nM, determined by SPR) to the S-protein and has been demonstrated to effectively neutralise SARS-CoV-2 *in vivo* (Zhou et al., 2020). Overall, the vast majority of Fab fragments analysed target the RBM, thus competing directly with hACE2, and those with higher binding affinities can neutralise Covid-19 virus *in vivo*. A recent study has evaluated the protection conferred by some of the Fab fragments herein analysed (Finkelstein et al., 2021). In it, the B38 Fab exhibited great post-infection efficacy in hACE2 transgenic mice, whilst the Fab fragments BD-368-2, CC12.1, S2E12 and S2M11 were also successful in protecting

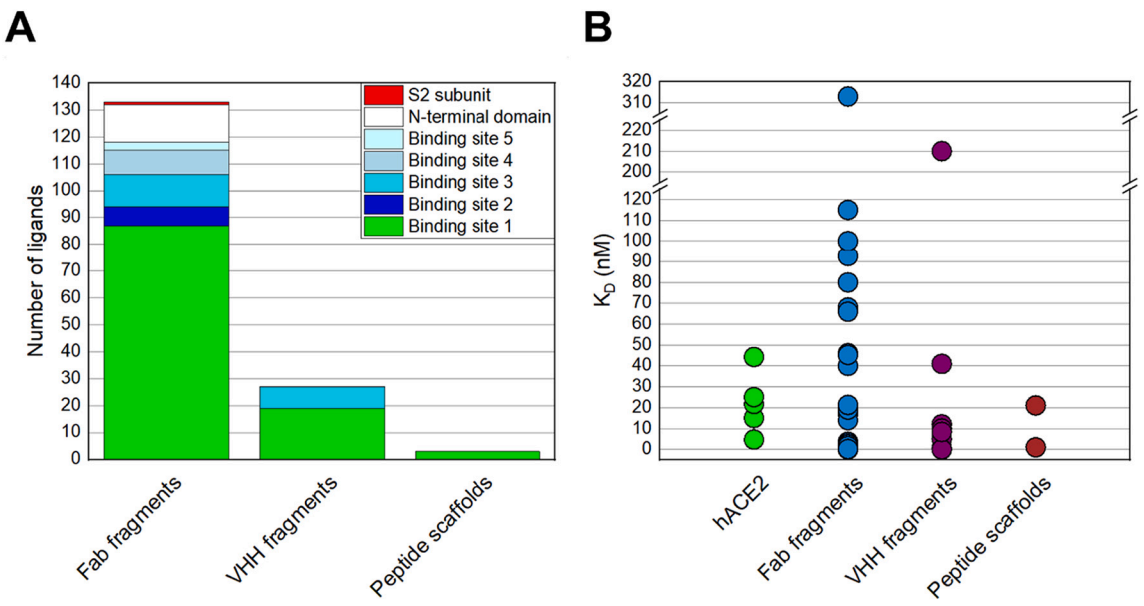

Fig. 6. **(A)** Distribution of all ligands whose structures were released in the PDB until mid-2021 per each of the S-protein binding sites herein identified. Those released after this point in time no longer impact on the tendency observed here. **(B)** Comparison between the dissociation constants (K_D) measured for the SARS-CoV-2 S-protein in complex with hACE2 and with the alternative ligands studied in more detail, specifically those whose structures were released until the 1st of January 2021.

hamsters against SARS-CoV-2. The BD-368-2, as well as H014, have even shown both prophylactic and therapeutic efficiency. In addition, the S2M11, S2H13 and S309 have been demonstrated to elicit antibody-dependent cellular cytotoxicity (ADCC), with S2M11 also eliciting antibody-dependent cellular phagocytosis (ADCP). Finally, a list of antibodies which have been approved for therapeutic use as of the time of writing can be consulted in Table 3, two of which (REGN10933 and REGN10987) have been reviewed here. Criteria used by health agencies to approve these antibodies included not only their high affinity towards the SARS-CoV-2 S-protein and proven efficiency in reducing infection, but also importantly their minimised negative side effects and longer residence time in the organism. Overall, these results highlight antibodies and Fab fragments as very promising therapeutic agents. More details regarding the Fab fragments, such as the dissociation constants, the fraction of the S-protein against which it was measured and the measurement methods are detailed in (Costa et al., 2021).

Regarding the shorter single-domain antibody fragments, these target RBD binding sites slightly more upstream the S-protein chain than most Fab fragments, albeit remaining within the RBM. The Ty1 VHH fragment (PDB 6ZXN), for instance, which does not interact with RBM residues 498–505, interacts with a greater number of RBM residues than even hACE2, unlike most of the Fab fragments analysed. At the time of writing, no data had yet been published on *in vivo* immunology assays with the single-domain antibody fragments considered in this review.

With the emergence of new SARS-CoV-2 variants, the risk of viral immune evasion increases. One approach to counter this is to develop multi-specific ligands, namely bispecific antibodies. These bispecifics have been isolated from llama VHH libraries, such as the Fu2-Ty1 VHH heterodimer, which has been demonstrated to effectively bind to two RBD simultaneously, albeit always in the same binding spot (binding spot 1), therefore requiring both RBD to be in the "up" conformation (Hanke et al., 2022). Alternatively, bispecific antibodies can be obtained through rational design by combining the Fabs of two different known antibodies. For instance, IgG-like CoV-X1 and CoV-X2 were designed based on two different natural antibodies. CoV-X1 combined antibody C135, which interacts with binding site 5, and antibody C144, which targets binding site 1; whilst CoV-X2 was based on C121, which interacts with binding sites 1 and 3, and also C135 (De Gasparo et al., 2021). Using this method, bispecific antibodies can even be designed to target other S-protein domains, whilst retaining one RBD-specific Fab. This is the case of CV1206_521_GS, which combines the Fabs of CV1206, a regular RBD-binding antibody, and CV521, which interacts with the S-protein NTD (Cho et al., 2021). At the time of writing, structures of the whole S-protein in complex with a bispecific antibody had not yet been

Table 3
Antibodies which have been approved for therapeutic use by April 2022 (Eurpean Medicines Agency, 2022; NIH, 2022).

Brand name	Developer and manufacturer	Name	K_D (nM)	PDB ID	Reference
Evusheld (tixagevimab/cilgavimab)	AstraZeneca	Tixagevimab (AZD8895)	0.253 (ELISA)	7L7E	(Dong et al., 2021)
		Cilgavimab (AZD1061)	<0.001 (ELISA)	7L7E	(Dong et al., 2021)
Regkirona	Celltrion	Regdanvimab (CT-P59)	0.027 (SPR)	7CM4	(Kim et al., 2021)
REGEN-COV or Ronapreve (casirivimab/imdevimab)	Regeneron; Roche as manufacturer outside the USA	Casirivimab (REGN10933)	0.0417 (ELISA)	6XDG	(Hansen et al., 2020)
		Imdevimab (REGN10987)	0.0428 (ELISA)	6XDG	(Hansen et al., 2020)
Xevudy	GlaxoSmithKline; Vir Biotechnology	Sotrovimab (VIR-7831, based on S309)	<0.001 (SPR)	7TLY	(McCallum et al., 2022)
Bamlanivimab/etesevimab	AbCellera Biologics; Eli Lilly Junshi Biosciences; Eli Lilly	Bamlanivimab (LY-CoV555)	<0.001 (SPR)	7KMG	(Jones et al., 2021)
		Etesevimab (LY-CoV016; JS016; CB6)	2.49 ± 1.65 (SPR)	7C01	(Shi et al., 2020)

released.

In addition to antibody-based ligands, *de novo* designed peptides and proteins inhibiting the interaction between hACE2 and the S-protein have also been developed at a fast pace. In this context, two relevant pioneering works were described.

One line of research was based on engineering hACE2 decoys (Linsky et al., 2020), which are 160 residues-long scaffolds. For example, the decoy CTC-445.2 accurately replicates the hACE2 interface that interacts with the S-protein RBM. As it is based on the natural host receptor of the S-protein, it is extremely resilient against viral immune evasion and has been demonstrated to bind to the RBM with even higher affinity than hACE2. The authors presented a dissociation constant in the nanomolar range, which was further improved by 10-fold when using bivalent decoy designs. Furthermore, it has also been shown to be able to bind to all three RBD simultaneously.

Another philosophy focused on the *de novo* design of S-protein ligands and was introduced by Baker's laboratory (Cao et al., 2020a). Two distinct approaches were followed. In the first approach, computer-generated scaffolds were built around the first α-helix of hACE2, where most contacts with the S-protein occur. In a second approach, computer-generated scaffolds were docked against an RBD structure and adjusted to optimise ligand sequence and conformation to yield the highest binding affinity. The best candidates resulting from both methods were subsequently produced and experimentally screened against the S-protein. Overall, binders obtained through the second approach were structurally stable and exhibited much higher binding affinities than those designed by the first approach, namely with K_D ranges of <1–20 nM for the former and 100–2000 nM for the latter, all measured using BLI (Cao et al., 2020a). Scaffolds LCB1 and LCB3, analysed in Table 2 and, in the case of the former, also Fig. 5G, were produced using the second approach. In a follow-up *in vivo* immunity assay by the same group, LCB1 has been demonstrated to confer substantial protection against SARS-CoV-2 in mice when administered intranasally up to 5 days prior to infection, even retaining its efficiency against the α variant (Case et al., 2021).

Finally, a third strategy sought the implementation of a non-antibody scaffold using ankyrin repeat protein (DARPin) technology to obtain a potent S-protein binder (Schilling et al., 2022; Rothenberger et al., 2021). DARPins typically consist of at least three ankyrin repeat motifs and have seen a growing interest in biopharma due to their versatility and remarkable binding affinities towards specific targets. Ensovibep is a five-motif DARPin designed against the S-protein. Out of its five covalently linked DARPin domains, three of them (R1, R2 and R3) bind the RBD of SARS-CoV-2 with picomolar affinity, whilst the other two (H1-H2) bind to human serum albumin (HSA), extending the ligand's systemic half-life. The protection conferred by Ensovibep has also been demonstrated *in vivo*, in which it effectively protected Roborovski dwarf hamsters from severe infection caused by wild type and α variant SARS-CoV-2, and it is, at the time of writing, undergoing late-stage clinical trials (Rothenberger et al., 2021).

These results indicate major possibilities for *de novo* designed ligands and non-antibody scaffolds, as well as the robustness of these ligands to develop novel therapies and vaccines that can be administered both by injection and intranasally (Table 4).

Table 4
Summary of the *in vivo* immunology assays using S-protein binders. The K_D values were measured against the S-protein.

Ligand type	Ligand name	K_D (nM)	*In vivo* results	References
Fab fragments	B38	1–100 (SPR)	Effectively reduced infection in hACE2-transgenic mice	(Finkelstein et al., 2021)
	BD-368-2	N/A	Prophylactic and therapeutic efficacy shown in hamsters	
	CC12.1	17 (BLI)	Effectively protected hamsters from infection	
	H014	N/A	Prophylactic and therapeutic efficacy shown in hamsters	
	S2E12	1.6–2.5 (SPR)	Effectively protected hamsters from infection	
	S2H13	N/A	Protected from infection and elicited ADCC	
	S2M11	0.2–68 (SPR)	Protected hamsters and elicited both ADCC and ADCP	
	S309	<0.001 (BLI)	Protected from infection and elicited ADCC	
De novo designed peptide scaffold	LCB1	<1 (BLI)	Administered intranasally up to 5 days before infection, effectively protected mice from wild-type and α variant SARS-CoV-2 infection	(Case et al., 2021)
Non-antibody scaffolds	DARPin	0.03–0.09 (SPR)	Effectively protected Roborovski dwarf hamsters from severe infection caused by wild type and α variant SARS-CoV-2	(Rothenberger et al., 2021)

3. Future perspectives

These are exciting times for peptide and protein engineers as we see the development of SARS-CoV-2 binders, mainly S-protein ligands, evolving daily. Protein engineering research can thus have an unprecedented global impact, accelerating the delivery of solutions to treat and prevent the Covid-19 pandemic. The fast pace at which scientists from different research fields provided fundamental insight about the biochemical and structural aspects of SARS-CoV-2 proteins is unheard-of, and it was critical for the prompt response from antibody and protein engineers to deliver selective and potent binders. These binders can be used as new diagnostic, prophylactic and therapeutic agents to treat and decrease the severity of the disease.

Several neutralising antibodies have been isolated from convalescent plasma and further characterised, the vast majority of which competing directly for the hACE2 binding site on the RBD. Interestingly, single-domain antibody fragments and *de novo* designed peptide scaffolds present the highest binding constants towards the S-protein – below 20 nM – which is in the same range as hACE2, the native binder. This shows the relevance of *in vitro* evolution methods and *in silico* studies to develop powerful affinity ligands against defined targets. Furthermore, it shows the versatility of non-antibody scaffolds (Gray et al., 2020; Dias et al., 2015; Dias et al., 2016; Dias and Roque, 2017; Batalha and Roque, 2016; Batalha et al., 2019) and the maturity of *de novo* protein design as a powerful tool to provide efficient binders in a short period of time. The Fab fragment sequences were obtained from full antibody sequences isolated from convalescent plasma and subsequently expressed in mammalian cell lines. In contrast, single-domain antibody fragments and *de novo* designed peptide scaffolds were typically expressed in bacterial hosts (*E. coli*), which significantly promotes fast and efficient ligand production to meet a worldwide demand. Moreover, non-antibody scaffolds are typically based on small and robust protein scaffolds with a high density of binding spots per molecule. These showed a high potential to provide non-invasive prophylactic and therapeutic solutions, namely through nasal administration (Case et al., 2021). However, considering the number of Fab fragments with promising *in vivo* results, it is likely that some will soon reach clinical trials phase and might effectively provide vaccines or therapeutic solutions for Covid-19. Finally, the virus will continue to evolve, as it was observed

for similar virus (MERS-CoV, SARS-CoV or H1N1 influenza) (Telenti et al., 2021). Thus, it will be necessary to maintain the vigilance over the structural variations in S-protein. Therefore, the research strategies reviewed in this work will be a blueprint for next generation ligands against SARS-CoV-2.

Declaration of Competing Interest

The authors declare no financial or commercial conflict of interest.

Acknowledgements

This work is funded by the European Union's Horizon 2020 programme under grant agreement No. 899732 (PURE Project), national funds from FCT – Fundação para a Ciência e a Tecnologia, I.P., in the scope of the project UIDP/04378/2020 and UIDB/04378/2020 of the Research Unit on Applied Molecular Biosciences – UCIBIO, the project LA/P/0140/2020 of the Associate Laboratory Institute for Health and Bioeconomy – i4HB, the projects PTDC/BII-BIO/28878/2017 (LISBOA-01-0145-FEDER-028878), PTDC/CTM-CTM/3389/2021 and the PhD fellowship of CFSC (2020.07566.BD).

References

Acharya, P., et al., 2020. A glycan cluster on the SARS-CoV-2 spike ectodomain is recognized by Fab-dimerized glycan-reactive antibodies. bioRxiv Prepr. Serv. Biol. https://doi.org/10.1101/2020.06.30.178897, 2020.06.30.178897.

Barnes, C.O., et al., 2020a. SARS-CoV-2 neutralizing antibody structures inform therapeutic strategies. Nature 588, 682–687.

Barnes, C.O., et al., 2020b. Structures of human antibodies bound to SARS-CoV-2 spike reveal common epitopes and recurrent features of antibodies. Cell 182, 828-842.e16.

Batalha, Í.L., Roque, A.C.A., 2016. Petasis-Ugi ligands: new affinity tools for the enrichment of phosphorylated peptides. J. Chromatogr. B Anal. Technol. Biomed. Life Sci. 1031, 86–93.

Batalha, I.L., Lychko, I., Branco, R.J.F., Iranzo, O., Roque, A.C.A., 2019. β-Hairpins as peptidomimetics of human phosphoprotein-binding domains. Org. Biomol. Chem. 17, 3996–4004.

Bertoglio, F., et al., 2021. SARS-CoV-2 neutralizing human recombinant antibodies selected from pre-pandemic healthy donors binding at RBD-ACE2 interface. Nat. Commun. 121577, 1–15.

Bissantz, C., Kuhn, B., Stahl, M., 2010. A medicinal chemist's guide to molecular interactions. J. Med. Chem. 53, 5061–5084.

Bracken, C.J., et al., 2020. Bi-paratopic and multivalent VH domains block ACE2 binding and neutralize SARS-CoV-2. Nat. Chem. Biol. 17, 113–121.

Cai, Y., et al., 2020. Distinct conformational states of SARS-CoV-2 spike protein. Science (80-.) 369 eabd4251.

Cao, L., et al., 2020a. De novo design of picomolar SARS-CoV-2 miniprotein inhibitors. Science (80-.) 370, 426–431.

Cao, Y., et al., 2020b. Potent neutralizing antibodies against SARS-CoV-2 identified by high-throughput single-cell sequencing of convalescent patients' B cells. Cell 182, 73–84.e16.

Case, J.B., et al., 2021. Ultrapotent miniproteins targeting the SARS-CoV-2 receptor-binding domain protect against infection and disease. Cell Host Microbe 29, 1151–1161.e5.

Chi, X., et al., 2020. A neutralizing human antibody binds to the N-terminal domain of the Spike protein of SARS-CoV-2. Science (80-.) 369, 650–655.

Cho, H., et al., 2021. Ultrapotent bispecific antibodies neutralize emerging SARS-CoV-2 variants Hyeseon. bioRxiv. https://doi.org/10.1101/2021.04.01.437942.

Costa, C., Barbosa, A.J., Dias, A.M.G., Roque, A.C.A., 2021. List of the Structures of S-Protein in Complex with Ligands Deposited in the Protein Data Bank until the 1st January 2021. https://doi.org/10.5281/ZENODO.5503855.

Costa, C., Barbosa, A.J., Dias, A.M.G., Roque, A.C.A., 2022. Analysis of the Interacting Residues between Wild Type SARS-CoV-2 Spike Protein and Natural Ligand hACE2, As Well as Three Engineered Alternative Ligands. https://doi.org/10.5281/ZENODO.6498918.

Custódio, T.F., et al., 2020. Selection, biophysical and structural analysis of synthetic nanobodies that effectively neutralize SARS-CoV-2. Nat. Commun. 11, 1–11.

De Gasparo, R., et al., 2021. Bispecific IgG neutralizes SARS-CoV-2 variants and prevents escape in mice. Nature. https://doi.org/10.1038/s41586-021-03461-y.

Dias, A., Roque, A., 2017. The future of protein scaffolds as affinity reagents for purification. Biotechnol. Bioeng. 114, 481–491.

Dias, A.M.G.C., Iranzo, O., Roque, A.C.A., 2015. An in silico and chemical approach towards small protein production and application in phosphoproteomics. RSC Adv. 5.

Dias, A.M.G.C., Dos Santos, R., Iranzo, O., Roque, A.C.A., 2016. Affinity adsorbents for proline-rich peptide sequences: a new role for WW domains. RSC Adv. 6, 68979–68988.

Dong, J., et al., 2021. Genetic and structural basis for SARS-CoV-2 variant neutralization by a two-antibody cocktail. Nat. Microbiol. 6, 1233–1244.

Du, S., et al., 2020. Structurally resolved SARS-CoV-2 antibody shows high efficacy in severely infected hamsters and provides a potent cocktail pairing strategy. Cell 183, 1013–1023.e13.

Du, L., Yang, Y., Zhang, X., 2021. Neutralizing antibodies for the prevention and treatment of COVID-19. Cell. Mol. Immunol. 18, 2293–2306.

Eurpean Medicines Agency, 2022. COVID-19 treatments | European Medicines Agency. https://www.ema.europa.eu/en/human-regulatory/overview/public-health-threats/coronavirus-disease-covid-19/treatments-vaccines/covid-19-treatments.

Finkelstein, M.T., et al., 2021. Structural Analysis of Neutralizing Epitopes of the SARS-CoV-2 Spike to Guide Therapy and Vaccine Design Strategies. https://doi.org/10.3390/v13010134.

Ghorbani, M., Brooks, B.R., Klauda, J.B., 2020. Critical sequence hotspots for binding of novel coronavirus to angiotensin converter enzyme as evaluated by molecular simulations. J. Phys. Chem. B 124, 10034–10047.

Gray, A., et al., 2020. Animal-free alternatives and the antibody iceberg. Nat. Biotechnol. 38, 1234–1238.

Han, P., et al., 2021. Molecular insights into receptor binding of recent emerging SARS-CoV-2 variants. Nat. Commun. 12, 1–9.

Hanke, L., et al., 2020. An alpaca nanobody neutralizes SARS-CoV-2 by blocking receptor interaction. Nat. Commun. 11, 1–9.

Hanke, L., et al., 2022. A bispecific monomeric nanobody induces spike trimer dimers and neutralizes SARS-CoV-2 in vivo. Nat. Commun. 13, 1–11.

Hansen, J., et al., 2020. Studies in humanized mice and convalescent humans yield a SARS-CoV-2 antibody cocktail. Science (80-.). 369, 1010–1014.

Hong, Q., et al., 2022. Molecular basis of SARS-CoV-2 Omicron variant receptor engagement and antibody evasion and neutralization. bioRxiv. https://doi.org/10.1101/2022.01.10.475532, 2022.01.10.475532.

Huang, Y., Yang, C., Xu, X. Feng, Xu, W., Liu, S. Wen, 2020. Structural and functional properties of SARS-CoV-2 spike protein: potential antivirus drug development for COVID-19. Acta Pharmacol. Sin. 41, 1141–1149.

Hurlburt, N.K., et al., 2020. Structural basis for potent neutralization of SARS-CoV-2 and role of antibody affinity maturation. bioRxiv. https://doi.org/10.1101/2020.06.12.148692, 2020.06.12.148692.

Jones, B.E., et al., 2021. The neutralizing antibody, LY-CoV555, protects against SARS-CoV-2 infection in nonhuman primates. Sci. Transl. Med. 13, 1906.

Ju, B., et al., 2020. Human neutralizing antibodies elicited by SARS-CoV-2 infection. Nature 584, 115–119.

Kim, C., et al., 2021. A therapeutic neutralizing antibody targeting receptor binding domain of SARS-CoV-2 spike protein. Nat. Commun. 12, 1–10.

Kreye, J., et al., 2020. A therapeutic non-self-reactive SARS-CoV-2 antibody protects from lung pathology in a COVID-19 Hamster model. Cell 183, 1058–1069.e19.

Lan, J., et al., 2020. Structure of the SARS-CoV-2 spike receptor-binding domain bound to the ACE2 receptor. Nature 581, 215–220.

Linsky, T.W., et al., 2020. De novo design of potent and resilient hACE2 decoys to neutralize SARS-CoV-2. Science (80-.) 370, 1208–1214.

Liu, L., et al., 2020a. Potent neutralizing antibodies against multiple epitopes on SARS-CoV-2 spike. Nature 584, 450–456.

Liu, H., et al., 2020b. Cross-neutralization of a SARS-CoV-2 antibody to a functionally conserved site is mediated by avidity. bioRxiv. https://doi.org/10.1101/2020.08.02.233536, 2020.08.02.233536.

Lv, Z., et al., 2020. Structural basis for neutralization of SARS-CoV-2 and SARS-CoV by a potent therapeutic antibody. Science (80-.) 369, 1505–1509.

Machhi, J., et al., 2020. The natural history, pathobiology, and clinical manifestations of SARS-CoV-2 infections. J. NeuroImmune Pharmacol. 15, 359–386.

Mannar, D., et al., 2022. SARS-CoV-2 omicron variant: antibody evasion and cryo-EM structure of spike protein–ACE2 complex. Science (80-.). https://doi.org/10.1126/SCIENCE.ABN7760.

McCallum, M., et al., 2022. Structural basis of SARS-CoV-2 omicron immune evasion and receptor engagement. Science. https://doi.org/10.1126/science.abn8652 eabn8652.

Moreira, R.A., Guzman, H.V., Boopathi, S., Baker, J.L., Poma, A.B., 2020. Characterization of structural and energetic differences between conformations of the SARS-CoV-2 spike protein. bioRxiv. https://doi.org/10.1101/2020.11.01.363499, 2020.11.01.363499.

NIH, 2022. Anti-SARS-CoV-2 monoclonal antibodies | COVID-19 treatment guidelines. In: COVID-19 Treatment Guidelines. National Institutes of Health. https://www.covid19treatmentguidelines.nih.gov/therapies/anti-sars-cov-2-antibody-products/anti-sars-cov-2-monoclonal-antibodies/.

Norman, A., et al., 2020. Discovery of cyclic peptide ligands to the SARS-CoV-2 spike protein using mRNA display. bioRxiv 2, 1–7.

Piccoli, L., et al., 2020. Mapping neutralizing and Immunodominant sites on the SARS-CoV-2 spike receptor-binding domain by structure-guided high-resolution serology. Cell 183, 1024–1042.e21.

Rath, S.L., Padhi, A.K., Mandal, N., 2021. Scanning the RBD-ACE2 molecular interactions in Omicron variant. bioRxiv. https://doi.org/10.1101/2021.12.12.472253, 2021.12.12.472253.

Renn, A., Fu, Y., Hu, X., Hall, M.D., Simeonov, A., 2020. Fruitful neutralizing antibody pipeline brings Hope to defeat SARS-Cov-2. Trends Pharmacol. Sci. 41, 815–829.

Rothenberger, S., et al., 2021. Ensovibep, a novel trispecific DARPin candidate that protects against SARS-CoV-2 variants. bioRxiv. https://doi.org/10.1101/2021.02.03.429164, 2021.02.03.429164.

Rujas, E., et al., 2020. Multivalency transforms SARS-CoV-2 antibodies into broad and ultrapotent neutralizers. bioRxiv 12, 1–12. https://doi.org/10.1038/s41467-021-23825-2, 2020.10.15.341636, 3661 In press.

Salvatori, G., et al., 2020. SARS-CoV-2 spike protein: an optimal immunological target for vaccines. J. Transl. Med. 18, 222.

Schilling, J., et al., 2022. Thermostable designed ankyrin repeat proteins (DARPins) as building blocks for innovative drugs. J. Biol. Chem. 298.
Schoof, M., et al., 2021. An ultrapotent synthetic nanobody neutralizes SARS-CoV-2 by stabilizing inactive spike. Science (80-.) 370, 1473–1479.
Scudellari, M., 2021. How the coronavirus infects cells - and why Delta is so dangerous. Nature 595, 640–644.
Shah, M., Woo, H.G., 2021. Omicron: a heavily mutated SARS-CoV-2 variant exhibits stronger binding to ACE2 and potently escape approved COVID-19 therapeutic antibodies. bioRxiv. https://doi.org/10.1101/2021.12.04.471200.
Shah, P., Canziani, G.A., Carter, E.P., Chaiken, I., 2021. The Case for S2: the potential benefits of the S2 subunit of the SARS-CoV-2 spike protein as an immunogen in fighting the COVID-19 pandemic. Front. Immunol. 12, 637651.
Shi, R., et al., 2020. A human neutralizing antibody targets the receptor-binding site of SARS-CoV-2. Nature 584, 120–124.
Telenti, A., et al., 2021. After the pandemic: perspectives on the future trajectory of COVID-19. Nature 596, 495–504.
Tortorici, M.A., et al., 2020. Ultrapotent human antibodies protect against SARS-CoV-2 challenge via multiple mechanisms. Science (80-.) 370, 950–957.
Veeramachaneni, G.K., Thunuguntla, V.B.S.C., Bobbillapati, J., Bondili, J.S., 2020. Structural and simulation analysis of hotspot residues interactions of SARS-CoV 2 with human ACE2 receptor. J. Biomol. Struct. Dyn. https://doi.org/10.1080/07391102.2020.1773318.
Wan, Y., Shang, J., Graham, R., Baric, R.S., Li, F., 2020. Receptor recognition by the novel coronavirus from Wuhan: an analysis based on decade-long structural studies of SARS coronavirus. J. Virol. 94.
Wang, Q., et al., 2020. Structural and functional basis of SARS-CoV-2 entry by using human ACE2. Cell 181, 894–904.e9.
Wang, P., et al., 2021a. Antibody resistance of SARS-CoV-2 variants B.1.351 and B.1.1.7. Nature. https://doi.org/10.1038/s41586-021-03398-2.
Wang, N., et al., 2021b. Structure-based development of human antibody cocktails against SARS-CoV-2. Cell Res. 31, 101–103.
Watanabe, Y., Allen, J.D., Wrapp, D., McLellan, J.S., Crispin, M., 2020. Site-specific glycan analysis of the SARS-CoV-2 spike. Science (80-.) 369, 330–333.
Williams, W.B., et al., 2021. Fab-dimerized glycan-reactive antibodies are a structural category of natural antibodies. Cell 184, 2955-2972.e25.
World Health Organization, 2021. WHO Coronavirus (COVID-19) Dashboard. WHO Coronavirus (COVID-19) Dashboard With Vaccination Data. WHO, pp. 1–5.
Wrapp, D., et al., 2020. Cryo-EM structure of the 2019-nCoV spike in the prefusion conformation. Science (80-.) 367, 1260–1263.
Wu, Y., et al., 2020a. A noncompeting pair of human neutralizing antibodies block COVID-19 virus binding to its receptor ACE2. Science (80-.) 368, 1274–1278.
Wu, N.C., et al., 2020b. An alternative binding mode of IGHV3-53 antibodies to the SARS-CoV-2 receptor binding domain. bioRxiv. https://doi.org/10.1101/2020.07.26.222232, 2020.07.26.222232.
Xiang, Y., et al., 2021. Versatile and multivalent nanobodies efficiently neutralize SARS-CoV-2. Science (80-.) 370, 1479–1484.
Yao, H., et al., 2021. Rational development of a human antibody cocktail that deploys multiple functions to confer Pan-SARS-CoVs protection. Cell Res. 31, 25–36.
Yoshimoto, F.K., 2020. The proteins of severe acute respiratory syndrome Coronavirus-2 (SARS CoV-2 or n-COV19), the cause of COVID-19. Protein J. 39, 198–216.
Yuan, M., et al., 2020a. A highly conserved cryptic epitope in the receptor binding domains of SARS-CoV-2 and SARS-CoV. Science (80-.) 368, 630–633.
Yuan, M., et al., 2020b. Structural basis of a shared antibody response to SARS-CoV-2. Science (80-.) 369, 1119–1123.
Zahradník, J., et al., 2021. SARS-CoV-2 variant prediction and antiviral drug design are enabled by RBD in vitro evolution. Nat. Microbiol. 6, 1188–1198.
Zhang, C., et al., 2021. Development and structural basis of a two-MAb cocktail for treating SARS-CoV-2 infections. Nat. Commun. 12, 6–9.
Zhou, D., et al., 2020. Structural basis for the neutralization of SARS-CoV-2 by an antibody from a convalescent patient. Nat. Struct. Mol. Biol. 27, 950–958.
Zhu, N., et al., 2020. A novel coronavirus from patients with pneumonia in China, 2019. N. Engl. J. Med. 382, 727–733.